STAR Protocols

CellPress
OPEN ACCESS

Protocol

Protocol for the purification and transcriptomic analysis of mouse astrocytes using GFAT

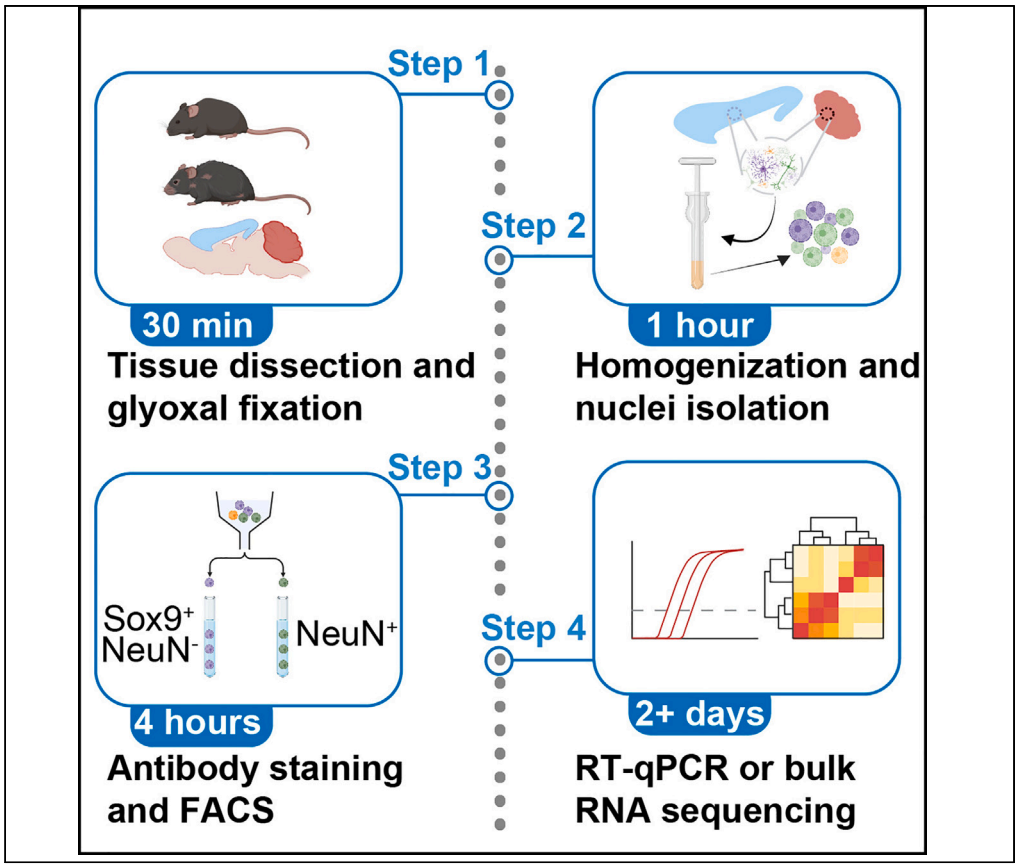

Astrocytes are glial cells of the central nervous system that modulate neuronal function. Here, we present glyoxal-fixed astrocyte nuclei transcriptomics (GFAT), a protocol for the purification and transcriptomic analysis of astrocyte nuclei from the cortex and cerebellum of adult and aged fresh mouse brain. We describe steps for tissue dissection, glyoxal fixation, homogenization, nuclei isolation, antibody staining, fluorescence-activated cell sorting, and RT-qPCR or bulk RNA sequencing. GFAT does not require transgenic lines or viral injection and allows parallel astrocyte and neuron profiling.

Publisher's note: Undertaking any experimental protocol requires adherence to local institutional guidelines for laboratory safety and ethics.

Lara Labarta-Bajo, James Deng, Minerva Contreras, Nicola J. Allen

nallen@salk.edu

Highlights

Purification and analysis of astrocyte nuclei with RT-qPCR and RNA-seq

Astrocyte transcriptomics across mouse models, brain regions, and ages

Parallel neuron profiling, which can uncover neuron-astrocyte crosstalk

Labarta-Bajo et al., STAR Protocols 4, 102599 December 15, 2023
https://doi.org/10.1016/j.xpro.2023.102599

STAR Protocols

CellPress
OPEN ACCESS

Protocol

Protocol for the purification and transcriptomic analysis of mouse astrocytes using GFAT

Lara Labarta-Bajo,[1,3] James Deng,[1,2] Minerva Contreras,[1,2] and Nicola J. Allen[1,3,4,*]

[1]Salk Institute for Biological Studies, La Jolla, CA 92037, USA

[2]Neurosciences Graduate Program, University of California, San Diego, La Jolla, CA 92093, USA

[3]Technical contact: llabartabajo@salk.edu, nallen@salk.edu

[4]Lead contact

*Correspondence: nallen@salk.edu
https://doi.org/10.1016/j.xpro.2023.102599

SUMMARY

Astrocytes are glial cells of the central nervous system that modulate neuronal function. Here, we present glyoxal-fixed astrocyte nuclei transcriptomics (GFAT), a protocol for the purification and transcriptomic analysis of astrocyte nuclei from the cortex and cerebellum of adult and aged fresh mouse brain. We describe steps for tissue dissection, glyoxal fixation, homogenization, nuclei isolation, antibody staining, fluorescence-activated cell sorting, and RT-qPCR or bulk RNA sequencing. GFAT does not require transgenic lines or viral injection and allows parallel astrocyte and neuron profiling.

BEFORE YOU BEGIN

Astrocytes are glial cells of the central nervous system that modulate the development, plasticity, and functionality of synapses in homeostasis[1] and in disease.[2] Mouse astrocytes are regionally heterogeneous[3–8] and can respond to the aging process in a location-specific manner.[6,7,9] Commonly used methods to profile astrocyte *in vivo* transcriptomes at high sequencing depth involve the use of transgenic mouse lines,[3,5–7] viral targeting of astrocytes,[10] enzymatic tissue digestion,[4] or nuclei purification with Fluorescence Activated Cell Sorting (FACS) based on LHX2,[11] which labels cortical but not cerebellar astrocytes in mice (Figure 6D), or based on PAX6,[12] which labels cortical and cerebellar astrocytes but also cerebellar neurons (Figure 6D). To enable the transcriptomic analysis of astrocytes across brain regions and mouse models we developed glyoxal-fixed astrocyte nuclei transcriptomics (GFAT), a protocol to obtain highly enriched astrocyte nuclei suspensions from fresh mouse cortex and cerebellum at two different chronological age ranges (3–6 and 20–24 months of age) without the need for transgenic mouse lines or viral injection. This methodology is structured in 4 major steps: 1) tissue dissection and brief fixation with the chemical glyoxal; 2) tissue homogenization and nuclei isolation; 3) antibody staining for transcription factors Sox9 (astrocytes) and NeuN (neurons) followed by FACS-purification; and 4) transcriptional analysis with reverse transcription quantitative real-time PCR (RT-qPCR) or transcriptomic analysis with bulk RNA sequencing (RNA-seq). This method is based on the detection of Sox9, an astrocyte-specific transcription factor in non-neurogenic regions across the CNS.[13] Prior work found detection of Sox9 by antibody labeling and immunofluorescence or FACS requires extensive fixation with paraformaldehyde (PFA) and prolonged incubation with primary antibody[13] (Figure 1), which negatively affects RNA quality and yield. To overcome this limitation and to simultaneously detect Sox9 within nuclei suspensions (Figure 2) and recover RNA suitable for transcriptomic analysis (Figure 5), we employ an alternative fixative, glyoxal, which preserves RNA quality similar to that of fresh tissue.[14] Using this approach, we show that astrocyte gene signatures are enriched, and oligodendrocyte and microglia genes are depleted, in $Sox9^{+}NeuN^{-}$ nuclei obtained with GFAT, independent of age or brain region analyzed

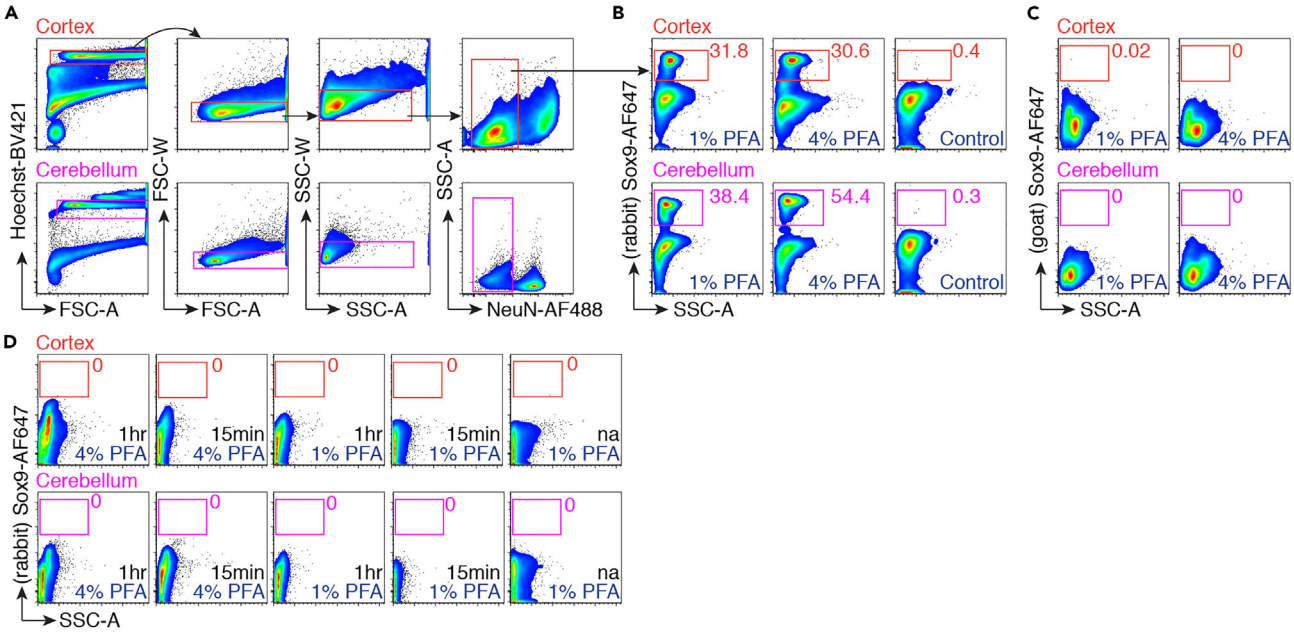

Figure 1. Detection of Sox9 by FACS in mouse cortical and cerebellar nuclei after extensive fixation with PFA and overnight staining with a specific primary antibody

(A) Adult (5 months old) WT C57BL/6 mice were anesthetized and transcardially perfused with 10 mL of 1X PBS, and 10 mL of 4% PFA. Cortex and cerebellum were dissected, minced, and submerged in 4% PFA solution for 22 h at 4°C. Nuclei suspensions were obtained and stained with Hoechst for 7 min, and with Alexa Fluor 488 (AF488)-conjugated mouse anti-NeuN for 22 h at 4°C. Our gating strategy was as follows: we plotted Hoechst against forward-scatter area (FSC-A) and gated on Hoechst$^+$ nuclei. Next, we gated single nuclei by drawing rectangle gates in FSC-A vs. FSC width (FSC-W) plots, and side-scatter area (SSC-A) vs. width (SSC-W) plots. Lastly, SSC-A vs. NeuN-AF488 plots were used to gate on non-neuronal (NeuN$^-$) nuclei, which contain astrocytes among other cell types. Gating strategy shown in A is representative of both 1% and 4% PFA samples and was used prior to gates shown in B-D. Pseudo-color FACS plots with a color gradient were used to represent the density of events within two-dimensional scatterplots. Low density values were assigned to cooler colors, such as blue or green, and high-density values were assigned to warmer colors like red or yellow.

(B and C) Adult (5 months old) WT C57BL/6 mice were anesthetized and transcardially perfused with 10 mL of 1X PBS, and 10 mL of 4% PFA ("4% PFA" and "Control" panels) or with 1% PFA ("1% PFA" panel). Cortex and cerebellum were dissected, minced, and submerged in 4% PFA ("4% PFA" and "Control" panels) or 1% PFA ("1% PFA" panel) solution for 22 h at 4°C. Nuclei suspensions were obtained and stained with Hoechst for 7 min, and with Alexa Fluor 488 (AF488)-conjugated mouse anti-NeuN together with (B) rabbit anti-Sox9 or (C) goat anti-Sox9 for 22 h at 4°C. Secondary staining was done with Alexa Fluor 647 (AF647)-conjugated secondary antibodies for 2 h on ice. A secondary antibody only control is included ('Control' panel). SSC-A vs. Sox9-AF647 plots were generated using NeuN$^-$ nuclei obtained in A, and gates were placed around Sox9$^+$ nuclei. Percentage of Sox9$^+$ nuclei among NeuN$^-$ single nuclei in cortex (orange gates) or cerebellum (pink gates) is shown.

(D) Adult (5 months old) WT C57BL/6 mice were anesthetized and transcardially perfused with 10 mL of 1X PBS, and 10 mL of 4% PFA ("4% PFA" panels) or with 1% PFA ("1% PFA" panels). Cortex and cerebellum were dissected, minced, and submerged in 4% PFA ("4% PFA" panels) or in 1% PFA ("1% PFA" panels) solution for 1 h or 15 min, as indicated. Some samples were not fixed further after perfusion (na). Nuclei suspensions were obtained and stained with Hoechst for 7 min, and with Alexa Fluor 488 (AF488)-conjugated mouse anti-NeuN together with rabbit anti-Sox9 for 2 h on ice. Secondary staining was done with Alexa Fluor 647 (AF647)-conjugated secondary antibodies for 2 h on ice. SSC-A vs. Sox9-AF647 plots were generated using NeuN$^-$ nuclei obtained as in A, and gates were placed around Sox9$^+$ nuclei. Percentage of Sox9$^+$ nuclei among NeuN$^-$ single nuclei in cortex (orange gates) or cerebellum (pink gates) is shown. Data shown are a representative experiment that has been repeated 2 times.

(Figures 6B and 6C). Overall, we provide an additional methodology to facilitate astrocyte-focused transcriptomic studies that can be applied across mouse models and brain regions.

Prepare ketamine/xylazine anesthetic

Timing: 20 min

Note: follow environmental health and safety guidelines of your institution regarding storage and handling of controlled substances.

1. Add 1.2 mL of ketamine and 1.2 mL xylazine to 10 mL of sodium chloride 0.9%.

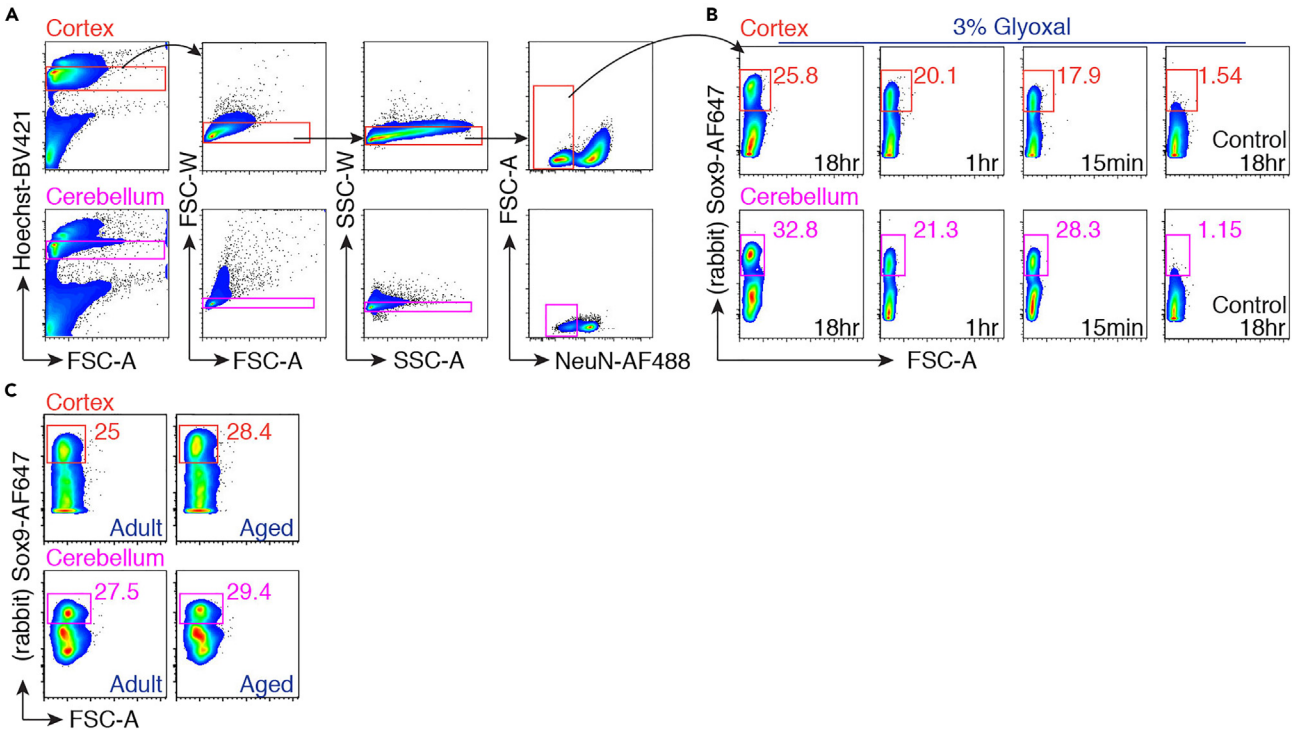

Figure 2. Detection of Sox9 by FACS after brief fixation with glyoxal in cortical and cerebellar nuclei from adult and aged mice

(A) Adult (4 months old) WT C57BL/6 mice were anesthetized and de-capitated. Cortex and cerebellum were dissected, minced and submerged in 3% glyoxal solution for 18 h on ice. Nuclei suspensions were obtained and stained with Hoechst for 7 min, and with Alexa Fluor 488 (AF488)-conjugated mouse anti-NeuN for 1 h on ice. Our gating strategy was as follows: we plotted Hoechst against FSC-A and gated on Hoechst$^+$ nuclei. Next, we gated single nuclei by drawing rectangle gates in FSC-A vs. FSC-W plots, and SSC-A vs. SSC-W plots. Lastly, SSC-A vs. NeuN-AF488 plots were used to gate on non-neuronal (NeuN$^-$) nuclei, which includes astrocytes. Gating strategy in A was used prior to gates shown in B, C. Pseudo-color FACS plots with a color gradient were used to represent the density of events within two-dimensional scatterplots. Low density values were assigned to cooler colors, such as blue or green, and high-density values were assigned to warmer colors like red or yellow.

(B) Adult (4 months old) WT C57BL/6 mice were anesthetized and de-capitated. Cortex and cerebellum were dissected, minced and submerged in 3% glyoxal solution for 18 h (“18 h” panels), 1 h (“1 h” panel) or 15 min (“15 min” panel) on ice. Nuclei suspensions were obtained and stained with Hoechst for 7 min, and with Alexa Fluor 488 (AF488)-conjugated mouse anti-NeuN together with rabbit anti-Sox9 for 1 h on ice. Secondary staining was done with Alexa Fluor 647 (AF647)-conjugated secondary antibodies for 1 h on ice. A secondary antibody only control is included for CTX and CB (‘Control’ panels). FSC-A vs. Sox9-AF647 plots were generated using NeuN$^-$ nuclei in A, and gates were placed around Sox9$^+$ nuclei. Percentage of Sox9$^+$ nuclei among NeuN$^-$ single nuclei in cortex (orange gates) or cerebellum (pink gates) is shown.

(C) Adult (4 months old) and aged (2 years old) WT C57BL/6 mice were anesthetized and de-capitated. Cortex and cerebellum were dissected, minced and submerged in 3% glyoxal solution for 15 min on ice. Nuclei suspensions were obtained and stained with Hoechst for 7 min, and with Alexa Fluor 488 (AF488)-conjugated mouse anti-NeuN together with rabbit anti-Sox9 for 1 h on ice. Secondary staining was done with Alexa Fluor 647 (AF647)-conjugated secondary antibodies for 1 h on ice. FSC-A vs. Sox9-AF647 plots were generated using NeuN$^-$ nuclei in A, and gates were placed around Sox9$^+$ nuclei. Representative plots show percentage of Sox9$^+$ nuclei among NeuN$^-$ single nuclei in cortex (orange gates) or cerebellum (pink gates) is shown. Data shown are a representative experiment that has been repeated more than 3 times.

2. Store at room temperature for up to 3 months.

Prepare 70% ethanol cleaning solution

Timing: 5 min

3. For every 500 mL of solution, mix 350 mL of ethanol (cleaner grade) with 150 mL ultrapure water.
4. Place in a plastic spray bottle.

Prepare sucrose 1 M

Timing: 10 min

Note: Store at 4°C for up to 6 months

5. Weigh 17.115 g of sucrose and place inside glass bottle containing 50 mL of ddH_2O and a stirring magnet.
6. Stir at room temperature until dissolved.

Prepare 10% Triton X-100 solution

Timing: 5 min

Note: Store at room temperature for up to 6 months

7. Take 500 µL of Triton X-100 stock and mix with 4.5 mL of ddH_2O (molecular grade).
8. Vortex thoroughly to mix.

Prepare nuclei isolation media (NIM)

Timing: 15 min

Note: Store at 4°C for up to 6 months

9. Mix the following reagents:

Reagent	Final concentration	Amount
Sucrose (1 M)	250 mM	12.5 mL
KCl (1 M)	25 mM	1.25 mL
$MgCl_2$ (1 M)	5 mM	0.25 mL
Tris-Cl pH 8.0 (1 M)	10 mM	0.5 mL
ddH_2O (molecular grade)	N/A	36.5 mL
Total	**N/A**	**50 mL**

Prepare diluent buffer

Timing: 15 min

Note: Store at 4°C for up to 6 months.

10. Mix the following reagents:

Reagent	Final concentration	Amount
Tris-Cl pH 8.0 (1 M)	120 mM	6 mL
KCl (1 M)	150 mM	7.5 mL
$MgCl_2$ (1 M)	30 mM	1.5 mL
ddH_2O (molecular grade)	-	35 mL
Total	-	**50 mL**

Prepare 50% iodixanol solution

Timing: 5 min

Note: Store at 4°C for up to 6 months.

Note: Recipe specifies amount of buffer required per sample

11. Mix 4 mL iodixanol with 0.8 mL of Diluent buffer.

Prepare 25% iodixanol solution

Timing: 5 min

Note: Store at 4°C for up to 6 months.

Note: Recipe specifies amount of buffer required per sample.

12. Mix 1.5 mL 50% iodixanol solution with 1.5 mL NIM.

Prepare 3% glyoxal acidic solution

Timing: 15 min

Note: Glyoxal stock solution should be handled inside a fume hood.

Note: Prepare fresh solution on the day of the experiment, do not store.

Note: Recipe specifies amount of buffer required per sample.

Note: White precipitate may appear over time in glyoxal (40% w/v) stock. To re-dissolve, place bottle on a hot plate set to 58°C and stir for 1 h. Once a completely clear solution is observed, let it cool down to room temperature before replacing at 4°C.

13. Mix the following reagents:

Reagent	Final concentration	Amount
Ethanol (absolute, molecular grade)	20%	0.789 mL
Glyoxal (40% w/v)	3% w/v	0.313 mL
Acetic acid (>99%)	0.75%	0.03 mL
NaOH (10 M)	5 mM	0.02 mL
ddH_2O (molecular grade)	-	2.835 mL
Total	-	**4 mL**

14. pH should be between 4 and 5. Adjust with additional NaOH if necessary.

Prepare nuclei isolation media supplemented with Triton (NIM-T)

Timing: 15 min

Note: Prepare fresh solution on the day of the experiment, do not store.

Note: Recipe specifies amount of buffer required per sample.

15. Mix the following reagents:

Reagent	Final concentration	Amount
NIM	-	3.462 mL
Triton X-100 (10% w/v in ddH_2O)	0.1%	35 μL
DTT (1 M)	1 mM	3.5 μL
Total		**3.5 mL**

16. Add 3 mL of NIMT solution into Dounce homogenizer and place on ice.

Prepare 1X PBS/1% BSA buffer

Timing: 10 min

Note: Store at 4°C for up to 6 months

Note: 0.2–1 U/mL of RNase inhibitor can be added to this buffer if performing RNA-seq.

17. Weigh 0.5 g BSA and add to 50 mL 1X DPBS.
18. Vortex until BSA is dissolved.

Prepare 2 mM Hoechst solution

Timing: 5 min

Note: Recipe is suitable to stain up to 20 samples.

Note: Prepare fresh solution on the day of the experiment, do not store.

19. Add 5 μL Hoechst (Thermo Fisher Scientific) stock to 45 μL 1X PBS/1% BSA.
20. Vortex briefly to mix.

Prepare primary antibody solution

Timing: 5 min

Note: Prepare fresh solution on the day of the experiment, do not store.

21. Prepare 50 μL per sample of rabbit anti-Sox9 (Abcam, 1:100 dilution) and mouse anti-NeuN-Alexa Fluor 488 (EMD Millipore, 1:1000 dilution) in 1X PBS/1% BSA.

Note: Given the large dilution factor of NeuN antibody, we recommend mixing 0.5 μL in 495.5 μL 1X PBS/1% BSA, then supplement with Sox9 the volume required for staining.

Note: After testing 2 different antibodies specific for Sox9, we found that only the rabbit clone EPR14335-78 (Abcam), but not the goat polyclonal antibody (R&D Systems) detects this protein by FACS after extensive fixation with PFA (Figure 1B). Since the goat antibody gave a negative result (Figure 1C), we proceeded to optimize GFAT using only the rabbit anti-Sox9 antibody.

Note: If a staining control for Sox9 needs to be included, prepare Primary Antibody solution with only mouse anti-NeuN-Alexa Fluor 488 (EMD Millipore), and without anti-Sox9 antibody.

Prepare secondary antibody solution

Timing: 5 min

Note: Prepare fresh solution on the day of the experiment, do not store.

22. Prepare 50 µL per sample of goat anti-Rabbit-Alexa Fluor 647 (Invitrogen, 1:200 dilution) in 1X PBS/1% BSA.

Prepare coated collection tubes for FACS-purification

Timing: 5 min

Note: Prepare on the day of the experiment, do not store.

Note: Coated tubes are only required for FACS purification (step 3, "FACS-purification of $Sox9^{+}NeuN^{-}$ and $NeuN^{+}$ nuclei")

23. Add 300 µL of ice-cold 1X PBS/1% BSA into 1.6 mL micro-centrifuge tubes (one tube per cellular population of interest).
24. Close tubes and vortex for 10 s to coat tube walls.

Note: This volume of buffer in the collection tube is optimized for the collection of up to 500,000 nuclei with a 70 µm sorting nozzle. Set up additional tubes if sorting a larger number of nuclei.

Prepare RLT buffer

Timing: 5 min

Note: Prepare on the day of the experiment, do not store.

Note: Recipe specifies amount of buffer required per sample

25. Inside a fume hood, supplement 350 µL RLT buffer (RNeasy Micro Kit, QIAGEN) with 10 µL/mL of beta-mercaptoethanol.
26. Close tube, briefly vortex to mix.

Materials preparation

27. Label 50 mL conical tubes (1 per sample) and replace cap with a 100 µm cell strainer (Figure 3E).
28. Label 50 mL centrifuge tubes compatible with high-speed centrifugation (1 per sample).
29. Place pestle A and pestle B inside 15 mL conical tubes, and place on ice.
30. Set table-top centrifuge (Sorvall Legend Micro 21R Centrifuge) at 4°C and let cool.
31. Set floor centrifuge (Sorvall RC 6+, Thermo Fisher Scientific) at 4°C and let cool.

Institutional permissions

Mouse handling conformed to the requirements of the National Institutes of Health and the Institutional Animal Care and Use Guidelines of the Salk Institute for Biological Studies. 2-year-old WT C57BL/6 mice were obtained from the National Institute on Aging (NIA) rodent colony. 3 to 6-month-old adult WT C57BL/6 mice were obtained from Jackson laboratories or were bred in-house. Male and female mice were used, and all animals were housed for at least 2 weeks before experiments. Before using this protocol, readers will have to obtain relevant approval to use live animals by their institution.

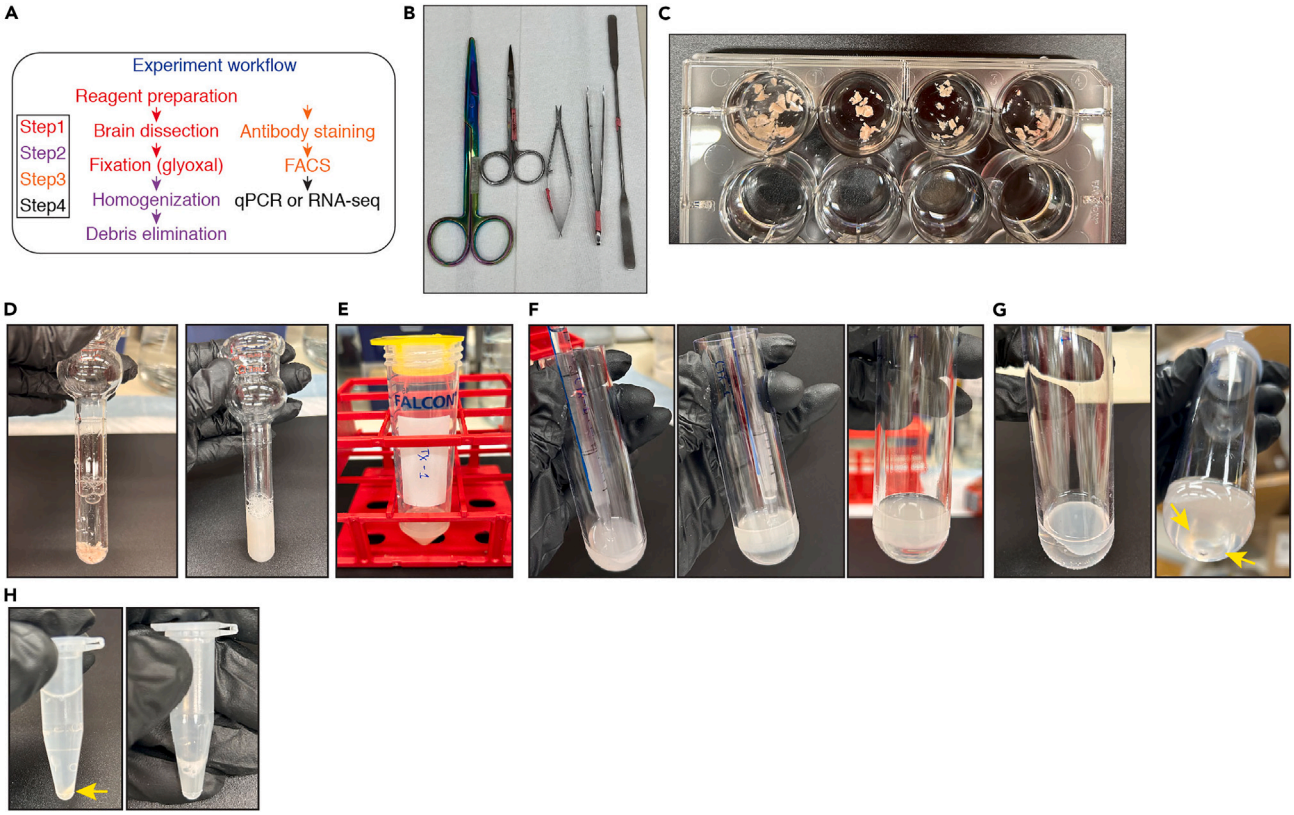

Figure 3. Tissue sample processing workflow

(A) Diagram summarizes the 4 steps of GFAT.

(B) Mouse dissection setup.

(C) Minced tissue pieces submerged in 4 mL of ice-cold glyoxal fixation solution.

(D) Tissue pieces are placed inside a Dounce homogenizer filled with 3 mL NIM-T solution (left) and are homogenized with pestles A and B (right).

(E) Tissue suspension is decanted through a 100 µm cell strainer and into a 50 mL tube.

(F) Place glass pipette at the bottom of a tube containing your tissue suspension supplemented with 50% iodixanol. Pipette 2.5 mL of 25% iodixanol very slowly. 2 density layers should be observed.

(G) After centrifugation, a top layer of debris (left) and a nuclear pellet (right, yellow arrows) will be observed.

(H) A white nuclei pellet should be observed after each centrifugation step. Example of a well-resuspended nuclei pellet in antibody solution is shown on the right.

KEY RESOURCES TABLE

REAGENT or RESOURCE	SOURCE	IDENTIFIER
Antibodies		
Rabbit anti-Sox9, clone EPR14335-78 (1:100 dilution)	Abcam	AB185966, RRID: AB_2728660
Goat anti-Sox9, polyclonal (1:100 dilution)	R&D Systems	AF3075
Donkey anti-goat IgG (H + L) cross-adsorbed secondary antibody, Alexa Fluor 647 (1:200 dilution)	Invitrogen	A-21447
Goat anti-rabbit IgG (H + L) highly cross-adsorbed secondary antibody, Alexa Fluor 647 (1:200 dilution)	Invitrogen	A-11034
Mouse anti-NeuN antibody, clone A60, Alexa Fluor 488 conjugated	EMD Millipore	MAB377X, RRID: AB_2149209
Chemicals, peptides, and recombinant proteins		
Hoechst 33342 solution (20 mM)	Thermo Fisher Scientific	62249
Recombinant RNase inhibitor	Takara	2313A
Ketamine hydrochloride injection (100 mg/mL)	Dechra	NDC 17033-100-10

(*Continued on next page*)

Continued

REAGENT or RESOURCE	SOURCE	IDENTIFIER
AnaSed injection (xylazine injection) sterile solution 20 mg/mL	Akorn	NDC 59399-110-20
0.9% sodium chloride, preservative-free	Hospira	NDC 0409-1918-32
Ethanol, absolute (200 proof), molecular biology grade, Fisher BioReagents	Fisher Scientific	BP2818100
Koptec pure ethanol (200 proof), cleaner grade	Decon Labs	V1001
Glyoxal solution	MilliporeSigma	128465
Acetic acid (>99%)	MilliporeSigma	A6283
Sodium hydroxide solution (10 M)	MilliporeSigma	72068
UltraPure DNase/RNase-free distilled water	Thermo Fisher Scientific	10977015
MilliporeSigma MQuant pH test strips and indicator papers	Fisher Scientific	M1095350007
Tris-HCl, 1 M solution, pH 8.0, molecular biology grade, UltraPure, Thermo Scientific Chemicals	Thermo Fisher Scientific	J22638.AE
Potassium chloride solution (1 M in ddH_2O)	MilliporeSigma	60142
Magnesium chloride solution (1 M in ddH_2O)	MilliporeSigma	63069
Sucrose, 99%	Thermo Fisher Scientific	A15583.0E
Triton X-100 (electrophoresis), Fisher BioReagents	Fisher Scientific	BP151-100
DL-dithiothreitol solution	MilliporeSigma	646563
OptiPrep (Iodixanol) density gradient medium	STEMCELL Technologies	07820
DPBS, no calcium, no magnesium (1X PBS)	Thermo Fisher Scientific	14190144
Bovine serum albumin	MilliporeSigma	A7030
2-Mercaptoethanol	MilliporeSigma	M3148
RNaseOUT Recombinant Ribonuclease Inhibitor	Thermo Fisher Scientific	10777019
Fast SYBR Green Master Mix	Thermo Fisher Scientific	4385612
Critical commercial assays		
RNeasy Micro Kit with RNase-free DNase I (50)	QIAGEN	74004
SuperScript IV VILO Master Mix	Thermo Fisher Scientific	11756050
Illumina Stranded Total RNA Prep with Ribo-Zero Plus	Illumina	20040525
Experimental models: Organisms/strains		
Mouse: C57BL/6J WT, male, 2 years old (aged) or C57BL/6J WT, male and female, 3–5 months old (adult)	Jackson Laboratory, National Institute on Aging (NIA)	000664
Oligonucleotides		
Rplp0 forward: GCTTCGTGTTCACCAAGGAGGA	IDT	N/A
Rplp0 reverse: GTCCTAGACCAGTGTTCTGAGC	IDT	N/A
Actb forward: AGGGAAATCGTGCGTGACAT	IDT	N/A
Actb reverse: GAACCGCTCGTTGCCAATAG	IDT	N/A
Aldh1l1 forward: CTTCATAGGCGGCGAGTTTGTG	IDT	N/A
Aldh1l1 reverse: CGCCTTGTCAACATCACTCACC	IDT	N/A
Gfap forward: CACCTACAGGAAATTGCTGGAGG	IDT	N/A
Gfap: reverse: CCACGATGTTCCTCTTGAGGTG	IDT	N/A
Mobp forward: TGCTGTGCCTGCCAGAAGACTA	IDT	N/A
Mobp reverse: TTGGCTTGGCTGGCATCAGAGG	IDT	N/A
Aif1 forward TCTGCCGTCCAAACTTGAAGCC	IDT	N/A
Aif1 reverse CTCTTCAGCTCTAGGTGGGTCT	IDT	N/A
Csf1r forward TGGATGCCTGTGAATGGCTCTG	IDT	N/A
Csf1r reverse GTGGGTGTCATTCCAAACCTGC	IDT	N/A
Software and algorithms		
FlowJo software	BD Biosciences	N/A
Prism GraphPad	GraphPad	N/A
Adobe Illustrator	Adobe	N/A
Other		
KIMBLE Dounce tissue grinder set (with pestle A and pestle B)	MilliporeSigma	D9063-1SET
Corning 100 μm cell strainer, yellow, sterile, individually packaged, 50/case	Corning	431752
BD FACSAria Fusion Flow Cytometer	BD Biosciences	N/A
Dumont #55 forceps	Fine Science Tools	11255-20

(*Continued on next page*)

Continued

REAGENT or RESOURCE	SOURCE	IDENTIFIER
QuantStudio 3 and 5 Real-Time PCR	Thermo Fisher Scientific	N/A
Spring scissors	Roboz	RS-5630
Perma-set scissors	Roboz	RS-6782
Light operating scissors	Roboz	RS-6752
Fisherbrand stainless steel lab spatula with PTFE coating	Fisher Scientific	13-820-057
Insulin syringe 1 mL (0.37 × 12.7 mm)	Comfort Point	26027
Falcon 100 mm × 15 mm not TC-treated bacteriological Petri dish	Corning	351029
Tissue culture plate, 12 well, flat bottom with low evaporation lid	Falcon	353043
Sorvall Legend micro 21R centrifuge	Thermo Fisher Scientific	N/A
Sorvall RC 6+ centrifuge	Thermo Fisher Scientific	N/A
Falcon 50 mL conical centrifuge tubes	Falcon	352070
1.6 mL graduated microcentrifuge tubes	Genesee Scientific	22-281
Nalgene high-speed polycarbonate round bottom centrifuge tubes	Thermo Fisher Scientific	3117-0120
Falcon 15 mL conical centrifuge tubes	Falcon	14-959-53A
Nalgene friction-fit polypropylene closures for plastic centrifuge tubes	Thermo Fisher Scientific	DS3111-0016
Serological pipette, 5 mL	Sigma	170355N
Adjustable single channel pipette, 100–1000 µL (P1000)	Eppendorf	SKU: 3123000063
Olympus Plastics 28-151, FACS tube, no cap, sterile 12 × 75 mm tubes (FACS tube)	Genesee Scientific	28-151

Alternatives: Standard reagents in this protocol, such as dissection tools, ethanol, salt solutions, plastics or oligonucleotides can be replaced by equivalent products from other manufacturers. Proprietary analysis and data representation tools listed (i.e. GraphPad or Adobe Illustrator) can be substituted with alternative, open source software. To ensure success with this protocol, we advise users to obtain glyoxal and iodixanol (OptiPrep) from the listed manufacturers, as other sources have not been tested.

STEP-BY-STEP METHOD DETAILS

Step 1) Brain dissection and glyoxal fixation

Timing: 30 min per mouse

This section describes the procedure to obtain brain regions of interest and fixation in glyoxal solution. An overview of the experimental workflow is included in Figure 3A.

1. Prepare mouse dissection area.
   a. Place absorbent pad and set aside large blunt scissors, fine forceps, spring scissors, and spatula (Figure 3B).
   b. Pre-fill one syringe per animal with 0.4 mL of anesthetic solution.
2. Pre-fill 12-well plate with 4 mL glyoxal solution per well (one well per tissue processed) (Figure 3A). Place all buffers and 12-well plate on ice.
   a. Obtain mouse of interest, administer 400 µL of anesthetic intraperitoneally. Wait until unresponsive to foot and tail pinch.
   b. Perform cervical dislocation, remove the head with large scissors, remove head skin and muscle with operating scissors and open the skull by inserting fine butterfly scissors posterior of the cerebellum.
      i. Cut along the midline and on each side of the brain.
      ii. Remove skull with fine forceps and obtain the brain with spatula.
   c. Place brain in petri dish containing ice-cold 1X PBS. Dissect cortex and cerebellum as fast as possible.
   d. Place each dissected brain region inside one well of a 12-well plate pre-filled with 4 mL of ice-cold glyoxal fixation solution.

i. Mince tissue with scissors into fragments of approximately 9 mm^3 in size (Figure 3C).
ii. Let plate with tissues sit on ice for 15 min.

Note: To prevent cross-contamination, clean scissors with 70% ethanol cleaning solution after each tissue is processed.

Note: If a large piece of tissue is being processed (e.g. a whole brain), fixation can be done in tubes. It is crucial that tissue is completely submerged in the fixative.

e. After 15 min, tilt plate at an angle of 45° and, with a P1000 pipette tip, remove as much glyoxal fixation solution as possible. Avoid removing tissue pieces.
f. Perform 2x washes with ice-cold PBS1X: add 4 mL of PBS1X and remove as much of it as possible, as detailed in step e. Repeat this twice. Fixed tissues are now ready for homogenization and obtention of nuclei.

Note: If processing several mice at a time, dissected tissues can be stored in ice-cold PBS1X and on ice for the length of the dissection. Fixation can be started once all tissues are gathered. We have successfully processed up to 16 tissue samples in parallel in this way.

Note: Prepare and dispose of anesthetics, and discard glyoxal fixative solution following your institution's environmental health and safety guidelines.

Note: To minimize the potential effects of acute hypoxia in the brain, it is recommended to use anesthesia rather than CO2 inhalation as the euthanasia procedure for this protocol.

Step 2) Tissue homogenization and nuclei isolation

Timing: 10 min per dissected tissue

This section outlines the process for obtaining nuclei from glyoxal-fixed tissue. This procedure involves two main steps: tissue homogenization and debris elimination using a density gradient with iodixanol.

3. Tissue homogenization.
   a. With forceps, transfer fixed and washed tissue pieces into Dounce homogenizer containing 3 mL NIM-T solution (Figure 3D).
   b. Use pestle A to homogenize tissue. Gently slide up and down 10 times or until tissue pieces are completely disaggregated. Replace pestle A.
   c. Repeat the previous step using pestle B. Replace pestle B. Homogenate should look like Figure 3D.
   d. Add 2 mL of 50% iodixanol to tissue suspension and mix 5 times with a P1000 pipette set to 500 µL.
4. Debris elimination and nuclei isolation.
   a. Decant suspension onto cell strainer in a 50 mL conical tube (Figure 3E). Tissue suspension should be filtered into the tube.
   b. Replace strainer with cap and place on ice.
   c. Transfer filtered tissue suspension into a high-speed centrifugation tube.

Note: Ensure that you carefully collect and transfer the entire sample, including any sample that may have splashed onto the walls of the tube.

   d. Load serological pipette with 2.5 mL 25% iodixanol and lower all the way to the bottom of the tube (Figure 3F-left).

e. Very slowly, dispense 2.5 mL of 25% iodixanol below the tissue suspension. 2 density layers should be observed (Figure 3F-center & right).

Note: Refer to troubleshooting section, problem 1, if 2 density layers are not observed.

f. Gently remove pipette to avoid disruption of the density gradient.
g. Spin down at 10,000 × *g* for 20 min at 4°C. Use floor centrifuge with a swinging rotor (Sorvall RC 6+, Thermo Fisher Scientific).

Note: After centrifugation, a pellet (nuclei) and debris in upper layers of the gradient should be observed (Figure 3G)

h. Discard supernatant containing debris.
i. Add 1 mL of ice-cold 1X PBS/1% BSA to the nuclei pellet and resuspend by pipetting 5 times with a P1000 pipette set to 0.5 mL.
j. Transfer nuclei suspension into a 1.6 mL micro-centrifuge tube. Place on ice.

Note: 1.6 mL micro-centrifuge tubes do not need to be coated for this step.

k. Use 10 μL of nuclei suspension for nuclei counting with a hemocytometer or cell counter.

Note: Refer to troubleshooting section, problem 2, if nuclei look very aggregated.

Step 3) Antibody staining and FACS

Timing: 4 h

This section details the procedure of antibody staining of nuclei suspensions and provides tips for FACS-purification of $Sox9^{+}NeuN^{-}$ and $NeuN^{+}$ nuclei.

5. Antibody staining of nuclei suspensions.
   a. Stain nuclei with Hoechst: add 2.5 μL of 2 mM Hoechst solution to each 1 mL of sample suspension. Close cap tightly, and invert tube 4 times. Place on ice for 7 min.
   b. Centrifuge at 1,000 × *g* for 5 min on a table-top centrifuge set at 4°C.

   Note: after centrifugation, a white pellet should be observed (Figure 3H). If processed tissue is too small, i.e., a specific cortical section, pellet may not be easily visible to the naked eye.

   c. Remove supernatant and add 50 μL of Primary Antibody solution. Mix with pipette 5–10 times.

   Note: Stain up to 5 × 10^{6} nuclei in 50 μL of Primary Antibody solution. Volume should be proportionally adjusted with larger number of nuclei.

   ⚠ CRITICAL: Make sure pellet is very well resuspended in Primary Antibody solution (Figure 3H, right).

   d. Place on ice for 1 h (protect tubes from light by covering ice bucket).
   e. Wash step: add 450 μL of 1X PBS/1% BSA and centrifuge at 1,000 × *g* for 5 min at 4°C.
   f. Remove supernatant. Add 50 μL Secondary Antibody solution. Mix with pipette 5–10 times.

   ⚠ CRITICAL: Make sure pellet is very well resuspended in Secondary Antibody solution.

   g. Place on ice for 1 h (protect tubes from light by covering ice bucket).

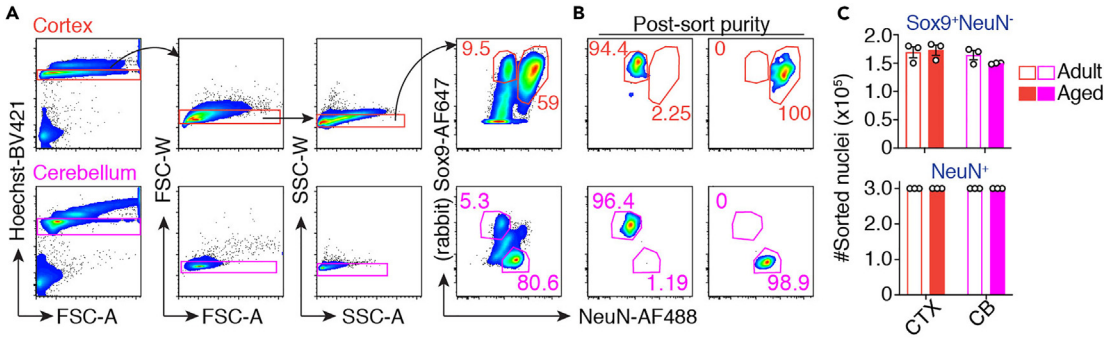

Figure 4. FACS-purification of Sox9$^+$NeuN$^-$ and NeuN$^+$ nuclei in cortex and cerebellum of adult and aged mice

(A–C) Adult (4 months old) and aged (2 years old) WT C57BL/6 mice were anesthetized and de-capitated, cortex and cerebellum were dissected, minced and submerged in 3% glyoxal solution for 15 min on ice. Nuclei suspensions were obtained and stained with Hoechst, anti-NeuN and anti-Sox9 primary and secondary antibodies. (A) Gating strategy to FACS-purify Sox9+NeuN- and NeuN+ nuclei in adult and aged cortex (CTX) and cerebellum (CB) was as follows: a Hoechst vs. FSC-A plot was used to gate Hoechst$^+$ nuclei, and single nuclei were gated in FSC-A vs. FSC-W, and SSC-A vs. SSC-W plots, as in Figure 2A. Lastly, NeuN vs. Sox9 plots were generated, and polygon gates were drawn around Sox9$^+$NeuN$^-$ and NeuN$^+$ nuclei. Gate numbers indicate the percentage of single nuclei that are Sox9$^+$NeuN$^-$ or NeuN$^+$. (B) To confirm post-sort nuclei purity, 10 μL of sorted nuclei suspension were added to 90 μL 1X PBS/1% BSA in a fresh FACS tube, and 50–150 events were recorded. Representative post-sort purity is shown; numbers indicate percentage of Sox9$^+$NeuN$^-$ or NeuN$^+$ among FACS-purified nuclei. (C) Number of sorted Sox9$^+$NeuN$^-$ and NeuN$^-$ nuclei in adult (empty bars) and aged (filled bars) cortex (CTX) and cerebellum (CB). (C) Error bars depict average ± standard error of the mean (SEM), data points mice (N = 3/group). Data shown are a representative experiment that has been repeated more than 3 times.

h. Wash step: add 450 μL of 1X PBS/1% BSA and centrifuge at 1,000 × *g* for 5 min at 4°C.
i. Remove supernatant. Re-suspend pellet in 500 μL of 1X PBS/1% BSA.
j. Use 10 μL of nuclei suspension for nuclei counting with a hemocytometer or cell counter.
k. Samples are ready for FACS-purification.

⚠ CRITICAL: Nuclei concentration for FACS-purification should be up to 5–10 × 10^6 nuclei/mL.

Note: If a staining control for Sox9 needs to be included, prepare Primary Antibody solution with only mouse anti-NeuN-Alexa Fluor 488 (EMD Millipore), and without anti-Sox9 antibody. Staining with Secondary Antibody solution should be performed normally, as described for non-control samples.

Note: Given that fluorescent properties of neuron nuclei can complicate astrocyte enrichment by FACS, it is recommended to always stain for both NeuN and Sox9, even if only astrocyte nuclei need to be purified. See discussion under limitations section, and Figure 8.

6. FACS-purification of Sox9$^+$NeuN$^-$ and NeuN$^+$ nuclei.

⚠ CRITICAL: Stained nuclei should be kept on ice at all times.

⚠ CRITICAL: Use coated collection tubes to maximize nuclei recovery after sorting

a. Set up BD FACSAria Fusion with a 70 μm nozzle.
b. Filter nuclei suspension through a 100 μm cell strainer and into a FACS tube right before sorting.
c. Sort Sox9$^+$NeuN$^-$ and NeuN$^+$ nuclei. Representative gating strategy for cortex and cerebellum is included in Figures 4A and 4B.
d. Collect purified nuclei into coated collection tubes placed in a collection tray set to 4°C. Place tubes on ice after sorting.

Note: Optimal flow rate for sample sorting on a BD FACS Aria Fusion is 7,000–10,000 events per second.

Note: The same gating strategy applies to 3–6 and 20–24-month-old mouse tissue (Figure 4A).

Note: To confirm post-sort nuclei purity add 10 μL of sorted nuclei suspension to 90 μL 1X PBS/1% BSA in a fresh FACS tube. Record 50–150 events (Figures 4B and 6C).

Note: It is expected to obtain $1.71 \times 10^5 \pm 1.44 \times 10^4$ (CTX) and $1.57 \times 10^5 \pm 1.2 \times 10^4$ (CB) $Sox9^+NeuN^-$, and at least 3×10^5 $NeuN^+$ nuclei from adult or aged mouse cerebellum or cortex (Figure 4C).

e. After all samples have been sorted, centrifuge collection tube at 1,000 × *g* for 5 min at 4°C in a table-top centrifuge.
f. Remove supernatant. 30–50 μL of supernatant can be left to avoid disrupting pellet

Note: Due to low nuclei numbers pellet may not be visible to the naked eye.

g. Add 350 μL of RLT buffer to each pellet. Vortex for 30 s to lyse nuclei, and store tubes at −80°C until ready for RNA extraction.

Note: Refer to troubleshooting section, problems 3, 4, and 5, if Hoechst or antibody staining are not observed or if frequent clogging occurs at the FACS.

Step 4) RT-qPCR or bulk RNA sequencing

Timing: 40 min (for step 7)

Timing: 1.5 h (for step 8)

Timing: 3–4 h (for step 9)

Timing: variable (for step 10)

Timing: variable (for step 11)

This section delineates the procedure to extract RNA from low amounts of sorted $Sox9^+NeuN^-$ or $NeuN^+$ nuclei, followed by recommendations to perform RT-qPCR and bulk RNA-seq. In addition, we provide a bulk RNA seq dataset of $Sox9^+NeuN^-$ and $NeuN^+$ nuclei in the adult and aged cortex and cerebellum, that was generated following the steps outlined below (Table S1).

7. RNA extraction.
   a. Obtain samples from −80°C freezer and thaw at room temperature for 10 min.
   b. Perform RNA extraction with the RNeasy Micro Kit following manufacturer's instructions and with the following optional steps:
      i. Perform on-column DNaseI digestion (following the manufacturer's instructions) to completely eliminate genomic DNA. In our experience, gDNA Eliminator columns (QIAGEN) are not sufficiently effective.
      ii. To increase RNA yields, perform elution step with 14 μL of molecular grade water previously warmed up to 65°C. Apply water to the center of the membrane inside the column, and let sit for 5 min before elution by centrifugation.

c. Store RNA at −80°C or directly proceed with next section.

8. Reverse transcription and quantitative PCR:
   a. Obtain RNA samples from −80°C and thaw on ice for 10 min.
   b. Perform reverse transcriptase (RT) reaction with Superscript IV VILO following manufacturer's instructions, and using 7 μL of total RNA.

SuperScript IV Vilo Master mix	4 μL
Template RNA	7 μL
Nuclease-free water	9 μL
Total reaction volume	20 μL

Note: RNA extracted from such number of nuclei (Figure 4C) is, in our experience, not reliably quantified with NanoDrop or Qubit. We advise microfluidic-based assays such as Bioanalyzer if absolute quantification is necessary.

   c. After RT reaction, cDNA can be stored at −20°C or used for subsequent quantitative PCR (qPCR).

9. qPCR from sorted astrocyte nuclei.

Note: Thaw SYBR Green PCR Master Mix on ice for 10 min.

Note: Obtain primers for genes of interest and for reference genes (Figure 5E).

   a. Set up qPCR reaction (volumes per well). Perform technical duplicates or triplicates per biological sample.

cDNA	0.4 μL
Nuclease-free water	4.04 μL
SYBR Green PCR Mastermix	5 μL
Forward primer (10 μM)	0.28 μL
Reverse primer (10 μM)	0.28 μL

   b. Run qPCR and melt curve analysis adjusted to primers of interest. The following cycling conditions were used in Figures 5F and 6C:

Steps	Temperature	Time	Cycles
AmpliTaq Fast DNA polymerase, UP activation	95°C	10 min	hold
Denaturation	95°C	15 s	40 cycles
Annealing & Extension	60°C	1 min	
Melt curve stage step 1	95°C	15 s	1
Melt curve stage step 2	60°C	1 min (ramp −1.6°C/sec)	1
Dissociation stage	95°C	15 s (ramp +0.075°C/sec)	1

10. RNA-seq library preparation and sequencing:
    Follow this methodology if RNA is intended for bulk RNA-seq
    a. This step can be performed right after RNA isolation, or with RNA samples that were previously stored at −80°C.

Note: Stored RNA samples should be thawed on ice for 10 min before the next step.

   b. Assess RNA quality and quantity with TapeStation (high sensitivity RNA tape) or Bioanalyzer following manufacturer's instructions.

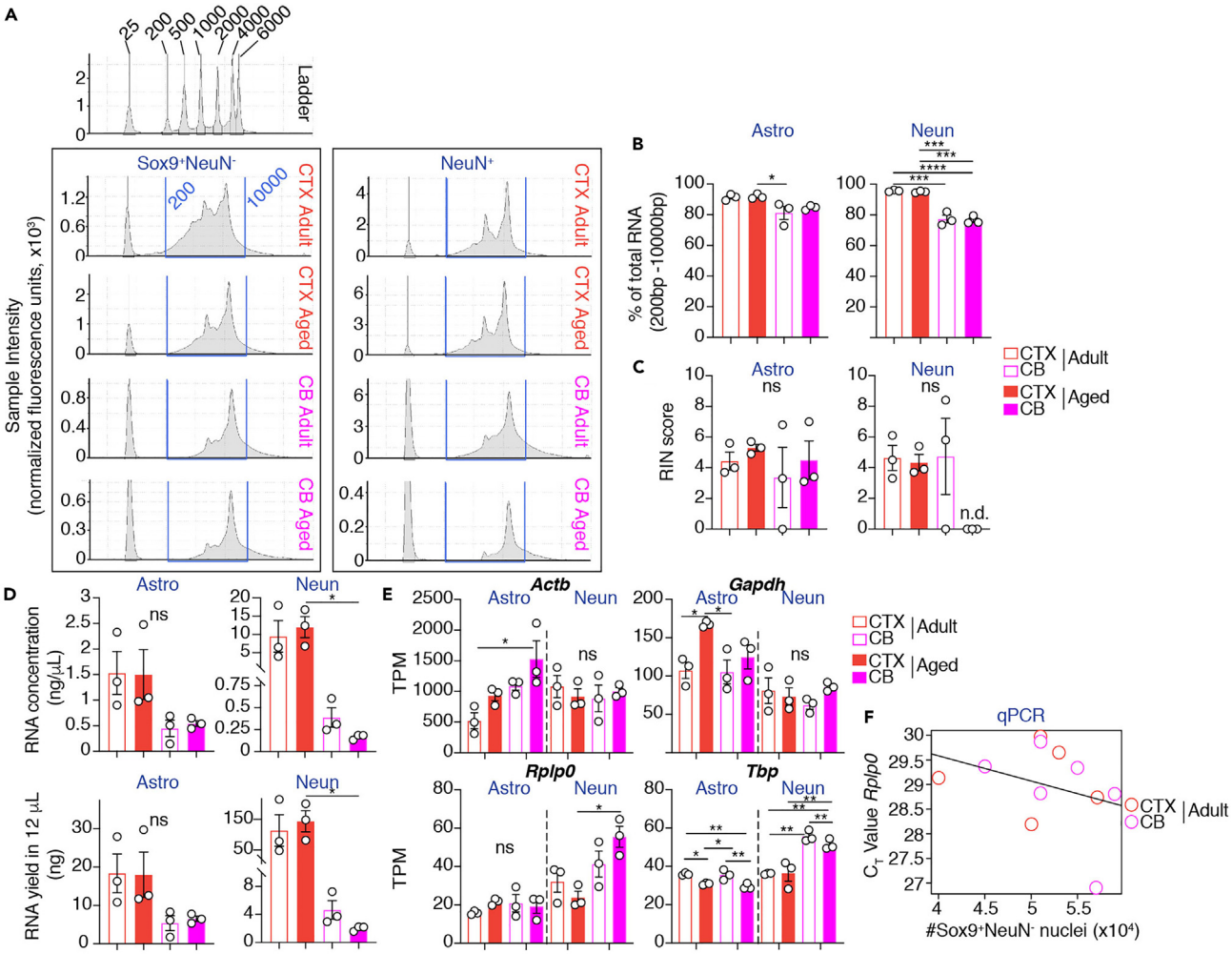

Figure 5. RNA recovered from Sox9$^+$NeuN$^-$ and NeuN$^+$ nuclei after glyoxal fixation is not highly fragmented and is suitable for qPCR amplification

(A–D) Sox9$^+$NeuN$^-$ and NeuN$^+$ nuclei were purified from adult and aged WT C57BL/6 mice as explained in Figure 4. RNA was extracted as specified in step 4 of the protocol. (A) Representative TapeStation traces for an RNA ladder and for each group. Blue lines indicate the size range used for DV200 analysis. Ladder scale units are nucleotides. Sample intensity (Y-axis) was scaled to the brightest value of fluorescence intensity for each plot. (B) Percentage of total RNA between 200 bp and 10000 bp in size after DV200 analysis and (C) RIN score. (D) RNA concentration was estimated with High Sensitivity RNA TapeStation and RNA yield was calculated by multiplying each sample concentration by 12 µL, which is the sample volume available after TapeStation analysis.

(E) Gene expression level of commonly used reference genes *Actb*, *Gapdh*, *Rplp0* and *Tbp* in Transcripts per Million (TPM). TPM values can be found under Table S1. F qPCR was performed with *Rplp0* primers in cortex and cerebellum Sox9$^+$NeuN$^-$ samples. Average cycle threshold (C_T) value (Y-axis) per number of FACS-purified nuclei (X-axis) is plotted. A regression line was added to the plot. Technical duplicates were employed for qPCR. (B) n.d. indicates RIN score was not possible to calculate. (B-E) Astro (Sox9$^+$NeuN$^-$ nuclei) or Neun (NeuN$^+$ nuclei). Black bars depict average ± standard deviation. One-way ANOVA with Tukey's multiple comparison correction: p-value <0.05*, <0.01**, <0.001***, <0.0001****, ns = not significant. Experiments shown were done with n = 3 mice/group (A-E) or n = 5–6 mice/group (F).

Note: The percentage of RNA fragments above 200 bp (DV200) can be estimated with TapeStation and is used to determine sample quality. Results of DV200 analysis show most RNA extracted is larger than 200 bp, which demonstrates minimal RNA fragmentation in all sample types (Figures 5A and 5B).

Note: The RNA concentration for each sample was estimated using TapeStation with high sensitivity RNA tape. For this assessment, 2 µL of each sample was utilized (Figure 5D, above). To determine the quantity of RNA available for library preparation, the RNA yield for each

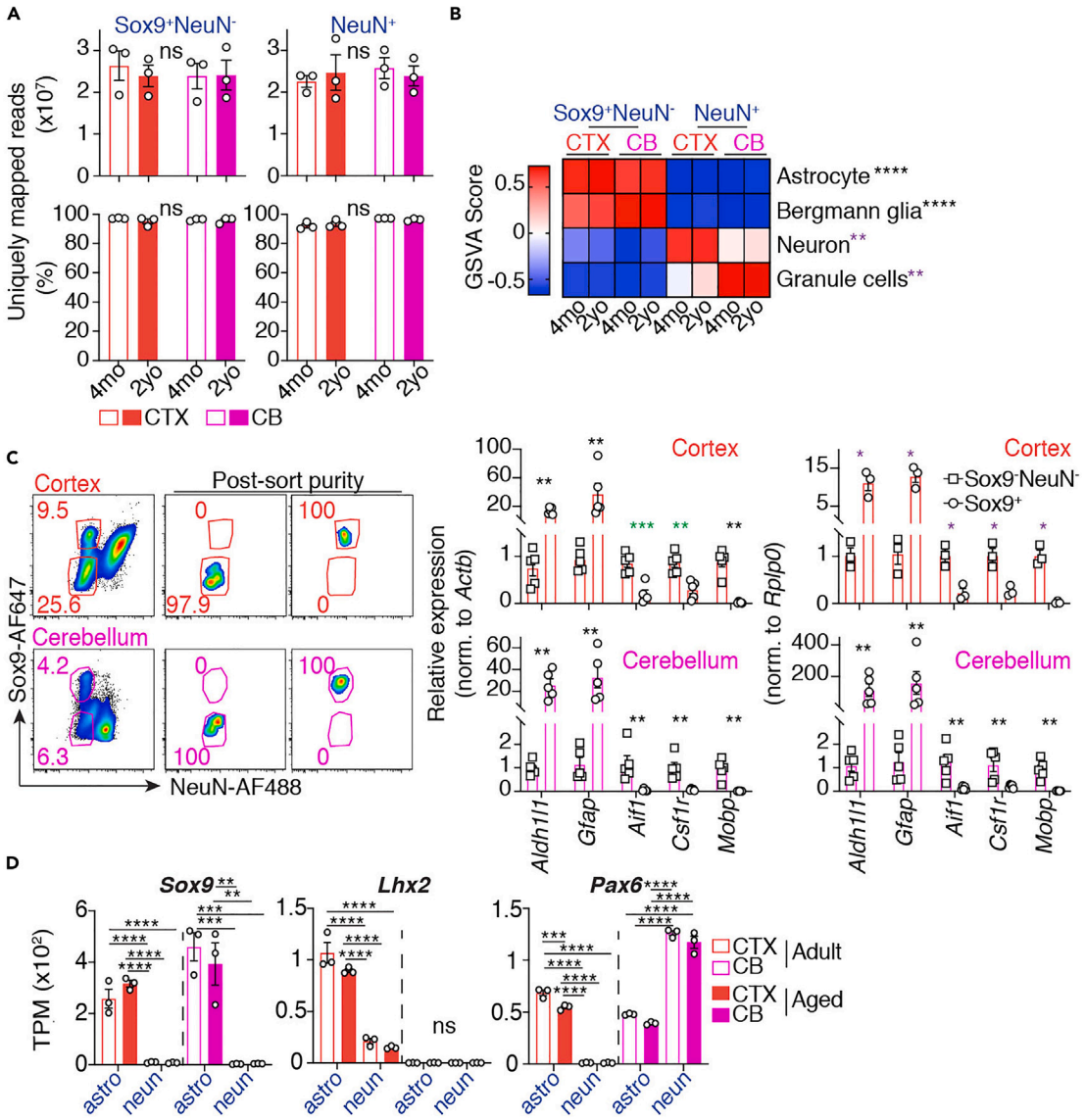

Figure 6. The GFAT method enriches for astrocytes in Sox9$^+$NeuN$^-$ nuclei fractions and neurons in NeuN$^+$ nuclei fractions

(A–D) (A, B, D) RNA-seq analysis of Sox9$^+$NeuN$^-$ and NeuN$^+$ nuclei obtained as detailed in Figure 4. (A) Absolute number (above) and percentage (below) of uniquely mapped sequencing reads after STAR (step 4). (B) Enrichment for astrocyte and neuron specific gene signatures was calculated using Gene Set Variation Analysis.[19] Average GSVA scores of 3 mice per condition are represented. High scores in red, represent positive enrichment, whereas low scores in blue represent lack of enrichment. Per sample scores and gene signatures are included in Tables S2 and S3. (C) Cortex (CTX) and cerebellar (CB) nuclei suspensions were obtained after glyoxal fixation from 3-month-old mice and were stained as detailed in Figure 4. Hoechst$^+$ and single nuclei were gated as detailed in Figure 4A. To FACS purify astrocytes and non-astrocytic, non-neuronal populations, gates were drawn around Sox9$^+$NeuN$^-$ and Sox9$^-$NeuN$^-$ nuclei, respectively. Post-sort nuclei purity for both populations was confirmed as in Figure 4B. After sorting, each sample underwent RNA extraction followed by RT-qPCR as detailed in step 4. For each biological sample, C_T values for each gene were double normalized to *Actb* or *Rplp0* C_T and to the average of the control group (Sox9$^-$NeuN$^-$ non-astrocytes) following the $2^{-\Delta\Delta CT}$ method. Sox9$^-$NeuN$^-$ samples are depicted with squares, and Sox9$^+$ astrocytes with circles. Technical duplicates were employed for qPCR analysis. (D) Gene expression level of *Sox9*, *Lhx2*, and *Pax6* is depicted in Transcripts per Million (TPM). Astro (Sox9$^+$NeuN$^-$ nuclei), Neun (NeuN$^+$ nuclei). (A, C, D) Error bars depict average ± standard error of the mean (SEM). (A, B, D) Statistical differences are shown with asterisks after One-way ANOVA with Tukey's multiple comparison correction (black), after Kruskal-Wallis test (violet) or (C) after *t*-test (green), Welch's *t*-test (violet) or Mann-Whitney test (black): p-value <0.05*, <0.01**, <0.001***, <0.0001****, ns = not significant. Experiments shown were done with n = 3 mice/group (A, B, D) or n = 3–5 mice/group (C).

sample was computed by multiplying sample concentration in ng/μL by 12 μL (Figure 5D, below). Note that 12 μL represents the volume of sample remaining after TapeStation analysis.

c. Construct libraries with the Illumina Stranded Total RNA prep (with Ribo-Zero Plus) sequencing kit, following manufacturer's instructions.

Note: Libraries can be constructed with equivalent amount of RNA for samples that will be directly compared after RNA-seq.

d. Sequence libraries.

Note: We have been successful with the following sequencing parameters: 2.5–3.5 × 10^7 reads per sample, paired end 100 bp reads on a NovaSeq S4.

11. Recommendations for RNA-seq data analysis.
    a. Quality control of sequenced reads with FastQC.[15]
    b. Map sequencing reads with STAR.[16] Select Mus musculus genome version mm10, obtain comprehensive gene annotation file from Gencode (GRCm38 assembly).
    c. Inspect mapping results with STAR (output log) and with the Integrative Genomics Viewer[17] to assess alignment quality.
    d. Count reads per genes with HOMER[18] analyzeRepeats command. Use '-count genes' option to count reads that map to introns and exons.

Note: Given that nuclei may contain a significant proportion of unspliced mRNA, it is advisable to include reads that map to introns in the analysis.

Note: Refer to troubleshooting section, problems 6, 7, and 8, if RNA yields or quality are lower than anticipated, or if C_T values for the reference gene are higher than expected (Figure 5F).

EXPECTED OUTCOMES

This protocol has been optimized for the purification of $Sox9^+NeuN^-$ and $NeuN^+$ nuclei in whole cortex and cerebellum from adult and aged WT C57BL/6 mice. It is expected that fixed and minced tissue pieces will look like in Figures 3C and 3D. Homogenization will result in a homogeneous and viscous suspension (Figure 3D) with no observable clumps after filtration (Figure 3E). Correct pipetting technique will result in visible separation between the lower 25% iodixanol and upper nuclear suspension phases (Figure 3F). After centrifugation, an upper layer of cellular debris and a white nuclei pellet should be observed (Figure 3G). A pellet should be observed in subsequent centrifugation steps (Figure 3H). Antibody staining protocol detailed in step 3 should yield $Sox9^+NeuN^-$ and $NeuN^+$ nuclei populations as depicted in Figures 4A and 4B. We typically recover 1.71 × 10^5 ± 1.44 × 10^4 and 1.57 × 10^5 ± 1.2 × 10^4 $Sox9^+NeuN^-$ nuclei from CTX and CB, irrespective of age (Figure 4C). As shown in Figure 4A (right panels), the $NeuN^+$ population is more abundant than $Sox9^+NeuN^-$ in both CTX and CB. As a result, 3 × 10^5 (or more) $NeuN^+$ nuclei can be obtained from each compartment at any of the ages tested (Figure 4C). RNA extraction as detailed in step 3 should result in TapeStation traces, RIN scores, concentrations and yields similar to Figures 5A–5D. Note that RIN scores rely on the detection of 18S and 28S rRNA, which are enriched in cytoplasm but not necessarily in nuclear fractions. In our experience, RNA yields and degree of fragmentation estimated with DV200 analysis (Figures 5B and 5D), rather than RIN scores (Figure 5C), are good predictors of the success of RNA-seq with this methodology. Of note, RNA yields are significantly lower in cerebellum neuron samples compared to the cortex (Figure 5D), even when obtained from similar nuclei numbers (Figure 4C), which may be a reflection of slightly higher RNA fragmentation in the former (Figure 5B). If qPCR from RNA in sorted $Sox9^+NeuN^-$ nuclei is performed, it is expected that cycle threshold (C_T) values for a reference gene such as *Rplp0* will fall within the 27–30 range, depending on the number of initial nuclei used for RNA extraction (Figure 5F). As a

result, number of input nuclei used for RNA extraction and qPCR should be adjusted according to the expected level of expression of the gene of interest. If RNA-seq is performed and analyzed as indicated in step 4, it is expected that sequence reads will be of good quality, as assessed with FastQC. After mapping with STAR, it is expected to obtain over 90% of uniquely mapped sequencing reads (Figure 6A-below), which should correspond to at least 1.78×10^7 reads per sample for subsequent analysis if sequencing recommendations in step 4 were followed (Figure 6A-above). To confirm that $Sox9^+NeuN^-$ and $NeuN^+$ nuclei express astrocyte and neuron gene signatures, respectively, Gene Set Variation Analysis (GSVA)[19] can be performed. GSVA summarizes expression values of genes belonging to a specific gene set into a single score. Using this analysis, it is expected to observe positive GSVA scores for astrocyte and Bergmann glia gene signatures in $Sox9^+NeuN^-$ nuclei, and negative scores for neuron genes at both ages analyzed. $NeuN^+$ nuclei should have positive scores for neuron signatures, and negative for astrocytes (Figure 6B; Tables S2 and S3). To further validate that GFAT enriches for astrocytes over other glial cell populations, we purified $Sox9^+NeuN^-$ (astrocytes) and $Sox9^-NeuN^-$ nuclei (Figure 6C), which is devoid of astrocytes and neurons and should contain other glia. Indeed, qPCR analysis showed significant enrichment for astrocyte markers *Aldh1l1* and *Gfap* in cortical and cerebellar $Sox9^+NeuN^-$ vs. $Sox9^-NeuN^-$, and enrichment for microglia genes *Aif1* and *Csf1r*, and for oligodendrocyte gene *Mobp* among $Sox9^-NeuN^-$ (Figure 6C). Overall, application of this methodology is expected to yield nuclei fractions highly enriched in astrocytes ($Sox9^+NeuN^-$) over other glia, or in neurons ($NeuN^+$), that can be used for downstream transcriptomic analysis.

QUANTIFICATION AND STATISTICAL ANALYSIS

A Shapiro-Wilk test was used to test for normality of the data. For comparisons between two groups of normally distributed data, a Fischer's test was used to compare variances. If variances were equal, we performed an unpaired two-tailed Student's t test. If variances were unequal, both a Welch's *t*-test and a Mann-Whitney test were conducted, and any observed differences were reported if identified by either test. If data were not normally distributed, a Mann-Whitney test was used. Significant differences among more than two groups of normally distributed data were determined with one-way ANOVA with Tukey's multiple comparison correction after confirming equal variances with a Brown-Forsythe test. If data were not normal or variances were unequal, a Kruskal-Wallis test was used. Statistical tests employed are detailed in each figure legend. Statistical analysis was performed with GraphPad Prism v8.

LIMITATIONS

We have validated this protocol in cortex and cerebellum of WT C57BL/6 mice. Pilot testing is advised if used in other brain regions, different ages or genetic backgrounds. This method may not be optimal in contexts where Sox9 is severely downregulated, as it relies on Sox9 protein expression. The method has been optimized in fresh brain tissue; we have observed lower percentage of $Sox9^+NeuN^-$ and dimmer Sox9 signal on a per-nucleus basis in fresh frozen adult CTX (Figure 7). Optimization of primary antibody concentration and/or staining time are warranted if working with fresh frozen tissues. In our experience, iodixanol gradient (step 2) is sufficient to remove myelin from cortex or cerebellum. An additional myelin depletion step may be required if working with highly myelinated regions of the central nervous system. After testing 2 different antibodies specific for Sox9, we found that rabbit anti-Sox9 (clone EPR14335-78) detects this protein by FACS after extensive fixation with PFA (Figure 1B). Given the negative result with polyclonal goat anti-Sox9 antibody (Figure 1C), we proceeded to optimize GFAT with only rabbit anti-Sox9. In addition, we were able to successfully detect NeuN after GFAT using the only antibody clone we tested (clone A60) (Figure 1A). It is possible that alternative antibodies are also compatible with this method, albeit pilot testing is advised. Fluorescent properties of neuron nuclei can influence this assay. We observed significantly higher granularity (represented by the SSC-A parameter) and increased fluorescence in the NeuN-AF488 and the Sox9-AF647 channels in cortical compared to cerebellar $NeuN^+$ nuclei (Figures 4A, 6C, and 8A–8D), in spite of similar Rbfox3 (NeuN) expression between groups and almost undetectable Sox9 transcript levels in cortical neuron nuclei (Figure 8E; Table S1). A similar observation was previously made (see Figure S1B in Nott et al.[11]). As a result, exclusion of $NeuN^+$

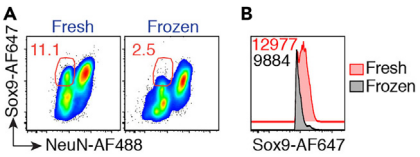

Figure 7. Detection of Sox9 by FACS after brief fixation with glyoxal in fresh or previously frozen cortical nuclei

(A and B) Whole cortex from both hemispheres was obtained from one adult C57BL/6 mouse. Each hemisphere was then placed in separate micro-centrifuge tubes and either stored on ice (fresh), or snap frozen in liquid nitrogen and thawed on ice for 20 min (frozen). Both samples were subsequently submerged in 3% glyoxal solution for 15 min. Nuclei suspensions were obtained and stained with Hoechst, anti-NeuN and anti-Sox9 primary and secondary antibodies. (A) Gating strategy was as follows: a Hoechst vs. FSC-A plot was used to gate Hoechst$^+$ nuclei, and single nuclei were gated in FSC-A vs. FSC-W, and SSC-A vs. SSC-W plots, as in Figure 4A (not shown). Lastly, NeuN vs. Sox9 plots were generated, and polygon gates were drawn around Sox9$^+$NeuN$^-$ nuclei. Gate numbers indicate the percentage of single nuclei that are Sox9$^+$NeuN$^-$ in fresh and frozen sample. (B) Mean fluorescence intensity values and histograms for Sox9 among gated Sox9$^+$NeuN$^-$ nuclei. Data shown are representative of an experiment that has been done 2 times.

nuclei is critical when aiming to enrich for astrocyte nuclei by FACS. qPCR analysis may not be feasible with less than 4 × 10^4 sorted Sox9$^+$NeuN$^-$ nuclei (Figure 5F), and RNA-seq may not be feasible with less than 1.45 × 10^5 Sox9$^+$NeuN$^-$ nuclei (Figure 4C). In that case, pooling of several mice per group is advised. Lastly, this method profiles nuclear RNA, which may not accurately represent mRNAs in the cytoplasm and astrocyte processes but can provide information on the current state of the cell and can potentially capture immediate transcriptional perturbation.

TROUBLESHOOTING

Problem 1

Density layers are not observed after 25% iodixanol is added to homogenized nuclei suspension (step 2).

Potential solution

If the amount of tissue processed is small it is possible that 2 layers are not easily observed due to low nuclei density in the upper layer. Proceed with centrifugation and, if a nuclei pellet is not clearly observed after centrifugation (step 2, "debris elimination and nuclei isolation"), carefully remove supernatant leaving up to 1 mL of iodixanol in the tube. Re-suspend nuclei pellet, transfer into a 1.6 mL micro-centrifuge tube and spin down at 1,000 × g for 5 min at 4°C in a table-top centrifuge. Remove supernatant down to 50 μL, re-suspend in 1 mL 1X PBS/1% BSA and proceed with Hoechst and antibody staining.

Problem 2

Nuclei look very aggregated under the microscope (step 2).

Potential solution

Highly aggregated nuclei can cause frequent clogging during the FACS-purification step. To avoid nuclei clumping, 1X PBS/1% BSA can be supplemented with EDTA at a final concentration of 1 mM, which should be used for staining and sorting.

Problem 3

Hoechst staining is not detected when running samples through the FACS (step 3).

Potential solution

This is likely due to improper re-suspension of nuclei in 1X PBS/1% BSA supplemented with Hoechst. Instead of inverting the tube, nuclei can be mixed 5 times with a P1000 pipette set to 500 μL.

Problem 4

NeuN staining is detected, but Sox9 is not, at the FACS (step 3).

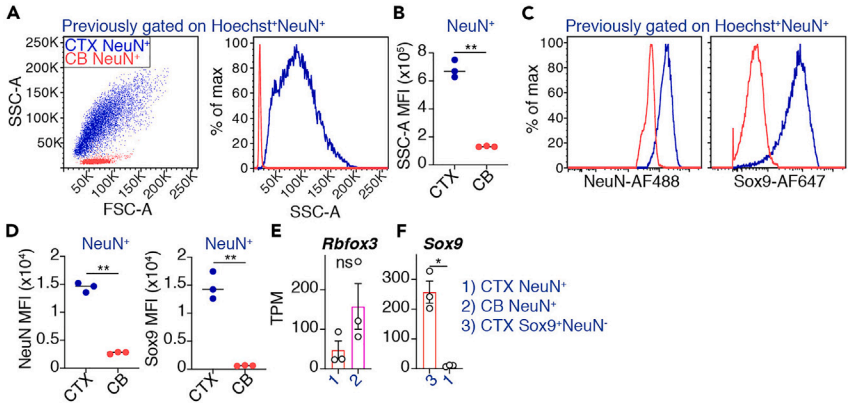

Figure 8. Higher granularity of NeuN$^+$ nuclei in the cortex compared to the cerebellum

(A–D) Adult (4 months old) WT C57BL/6 mice were anesthetized and de-capitated, cortex and cerebellum were dissected, minced and submerged in 3% glyoxal solution for 15 min on ice. Nuclei suspensions were obtained and stained with Hoechst, anti-NeuN and anti-Sox9 primary and secondary antibodies. (A) Gating strategy to analyze NeuN$^+$ nuclei in CTX and CB was as follows: a Hoechst vs. FSC-A plot was used to gate Hoechst$^+$ nuclei, and single nuclei were gated in FSC-A vs. FSC-W, and SSC-A vs. SSC-W plots, as in Figure 2A. Lastly, NeuN vs. Sox9 plots were generated, and polygon gates were drawn around NeuN$^+$ nuclei, as in Figure 4A. (A) FSC-A by SSC-A plots, SSC-A histograms, and (C) NeuN-AF488 or Sox9-AF647 histograms were generated with only NeuN$^+$ nuclei of the CTX (blue) and the CB (red). (B, D) Mean fluorescence intensity (MFI) for SSC-A, NeuN-AF488 and Sox9-AF647 parameters is plotted. (B, D) Black lines represent the mean.

(E and F) (E) Gene expression level of *Rbfox3* (encodes NeuN) and *Sox9* is shown for all samples in Transcripts per Million (TPM). TPM values can be found under Table S1. Numbers on the X-axis correspond to 1) NeuN$^+$ (neuron) nuclei of the CTX, 2) NeuN$^+$ (neuron) nuclei of the CB, or 3) Sox9$^+$NeuN$^-$ (astrocyte) nuclei of the CTX. (B, D, F) Welch's t-test, (F) : p-value <0.05*, <0.01**, (E) Mann-Whitney test: ns = not significant. Data shown are representative of an experiment that has been done more than 3 times (A-D). Experiment shown was done with n = 3 mice/group (E-F). (E, F) Error bars depict average ± standard error of the mean (SEM).

Potential solution

NeuN staining of nuclei with the antibody listed in this protocol works both on fresh[20] and fixed tissue (Figures 1A, 2A, 4A, and 6C), while Sox9 only works on fixed tissue (Figures 1B, 1D, 2B, 2C, 4A, and 6C). Weak or inexistent Sox9 stain, but positive NeuN stain, may indicate improper fixation due to several reasons; 1) 3% glyoxal solution was improperly prepared or was not made fresh on the day of the experiment, 2) tissue dissociation was insufficient, or tissue was not completely submerged in fixative. This prevents proper penetration of glyoxal solution. 3) Fixation step was performed for less than 15 min. Improving any of these steps should solve the problem.

Problem 5

Frequent clogging at the FACS (step 3).

Potential solution

Nuclei aggregation can occur before or during sorting. Make sure that the sample to be sorted is filtered through a 100 μm strainer right before loading at the FACS and re-filtered every 25 min of sorting. A nuclei concentration higher than 5–10 × 10^6 nuclei/mL and/or high event rates can also contribute to this issue. Dilute sample further. If problem persists, 85 μm or 100 μm nozzles can be used instead of a 70 μm. Lastly, as explained in problem 2, 1X PBS/1% BSA solution can be supplemented with 1 mM EDTA.

Problem 6

RNA yields are lower than expected.

Potential solution

To increase nuclei recovery during sorting, coat tubes as detailed in the 'before you begin' section. After sorting, samples can be spun down for 10 min (instead of 5) at 1,000 × *g* and 4°C. In preparation for RNA

extraction, vortex sample in RLT, and spin down for 1 min at 1,000 × *g* before starting QIAGEN RNeasy Micro kit protocol, to recover as much sample as possible. Lastly, note that for similar numbers of sorted nuclei (Figure 4C) the expected RNA yields are lower in CB compared to CTX (Figure 5D). It is possible that lower RNA yields in the CB are a consequence of slightly more fragmented RNA (Figures 5A and 5B) or may be a reflection of the biology of the brain region being studied.

Problem 7

RNA looks degraded and has low RIN scores by TapeStation analysis, is this problematic for RNA-seq analysis?

Potential solution

The Illumina Library preparation kit used in this protocol is optimized for 1–1000 ng purified total RNA input from high quality samples (RIN≥9) and accepts 10–100 ng RNA input from low quality samples (RIN ≥ 2) or formalin-fixed paraffin-embedded, as long as over 55% of the RNA is larger than 200 bp. Note that RIN scores rely on the detection of 18S and 28S rRNA, which are enriched in cytoplasm but not necessarily in nuclear fractions. In our experience, RNA yields and degree of fragmentation (Figures 5A, 5B and 5D), rather than RIN scores (Figure 5C), are a good predictor of the success with RNA-seq.

Problem 8

C_T values for the reference gene are higher than expected.

Potential solution

Increase number of initial nuclei used for RNA extraction, as C_T values are inversely proportional to the amount of initial sorted nuclei (Figure 5F). The amount of cDNA used per qPCR reaction can also be increased up to 4.44 μL with the proposed protocol, and reaction volume can be increased to 20 μL to accommodate a bigger volume of cDNA.

RESOURCE AVAILABILITY

Lead contact

Further information and requests for resources and reagents should be directed to and will be fulfilled by the lead contact, Nicola J Allen, nallen@salk.edu.

Materials availability

Individual materials required for this protocol are commercially available from sources specified in the key resources table.

Data and code availability

Data employed in Figure 6 are included under Tables S1, S2, and S3. All RNA-seq data have been deposited to the Gene Expression Omnibus (accession no. GSE233509).

SUPPLEMENTAL INFORMATION

Supplemental information can be found online at https://doi.org/10.1016/j.xpro.2023.102599.

ACKNOWLEDGMENTS

We thank members of the Allen Laboratory and Dr. Miguel Reina-Campos for helpful discussions. This work was supported by the Chan Zuckerberg Initiative to N.J.A. L.L.-B. is supported by a Hewitt Foundation Postdoctoral Fellowship. J.D. is supported by F30 HD106699 from the National Institute of Child Health and Human Development and a FRAXA Research Foundation Fellowship. M.C. is supported by the National Academies of Sciences, Engineering, and Medicine Ford Foundation Predoctoral Fellowship. This work was supported by the Flow Cytometry Core Facility of the Salk Institute (RRID: SCR_014839) with funding from NIH-NCI CCSG: P30 014195 and Shared Instrumentation Grant S10-OD023689 (Aria Fusion Cell Sorter). This publication includes data generated at the UC San Diego

IGM Genomics Center utilizing an Illumina NovaSeq 6000 that was purchased with funding from an NIH SIG grant (#S10 OD026929). We thank the Animal Resources Department at the Salk Institute. We thank the NIA for providing aged mice used in this study. The graphical abstract was created using BioRender.

AUTHOR CONTRIBUTIONS

L.L.-B. designed, performed, analyzed, and interpreted all experiments and wrote the manuscript. J.D. and M.C. independently validated the protocol and edited the manuscript. N.J.A. conceived and supervised the project, designed and interpreted experiments, and edited the manuscript.

DECLARATION OF INTERESTS

The authors declare no competing interests.

REFERENCES

1. Allen, N.J. (2014). Astrocyte regulation of synaptic behavior. Annu. Rev. Cell Dev. Biol. *30*, 439–463. https://doi.org/10.1146/annurev-cellbio-100913-013053.

2. Blanco-Suárez, E., Caldwell, A.L.M., and Allen, N.J. (2017). Role of astrocyte-synapse interactions in CNS disorders. J. Physiol. *595*, 1903–1916. https://doi.org/10.1113/JP270988.

3. Mazumder, A.G., Julé, A.M., Cullen, P.F., and Sun, D. (2022). Astrocyte heterogeneity within white matter tracts and a unique subpopulation of optic nerve head astrocytes. iScience *25*, 105568. https://doi.org/10.1016/j.isci.2022.105568.

4. Herrero-Navarro, Á., Puche-Aroca, L., Moreno-Juan, V., Sempere-Ferràndez, A., Espinosa, A., Susín, R., Torres-Masjoan, L., Leyva-Díaz, E., Karow, M., Figueres-Oñate, M., et al. (2021). Astrocytes and neurons share region-specific transcriptional signatures that confer regional identity to neuronal reprogramming. Sci. Adv. *7*, eabe8978. https://doi.org/10.1126/sciadv.abe8978.

5. Morel, L., Chiang, M.S.R., Higashimori, H., Shoneye, T., Iyer, L.K., Yelick, J., Tai, A., and Yang, Y. (2017). Molecular and Functional Properties of Regional Astrocytes in the Adult Brain. J. Neurosci. *37*, 8706–8717. https://doi.org/10.1523/JNEUROSCI.3956-16.2017.

6. Boisvert, M.M., Erikson, G.A., Shokhirev, M.N., and Allen, N.J. (2018). The Aging Astrocyte Transcriptome from Multiple Regions of the Mouse Brain. Cell Rep. *22*, 269–285. https://doi.org/10.1016/j.celrep.2017.12.039.

7. Clarke, L.E., Liddelow, S.A., Chakraborty, C., Münch, A.E., Heiman, M., and Barres, B.A. (2018). Normal aging induces A1-like astrocyte reactivity. Proc. Natl. Acad. Sci. USA *115*, E1896–E1905. https://doi.org/10.1073/pnas.1800165115.

8. Batiuk, M.Y., Martirosyan, A., Wahis, J., de Vin, F., Marneffe, C., Kusserow, C., Koeppen, J., Viana, J.F., Oliveira, J.F., Voet, T., et al. (2020). Identification of region-specific astrocyte subtypes at single cell resolution. Nat. Commun. *11*, 1220. https://doi.org/10.1038/s41467-019-14198-8.

9. Hajdarovic, K.H., Yu, D., Hassell, L.A., Evans, S., Packer, S., Neretti, N., and Webb, A.E. (2022). Single-cell analysis of the aging female mouse hypothalamus. Nat. Aging *2*, 662–678. https://doi.org/10.1038/s43587-022-00246-4.

10. Yu, X., Nagai, J., Marti-Solano, M., Soto, J.S., Coppola, G., Babu, M.M., and Khakh, B.S. (2020). Context-Specific Striatal Astrocyte Molecular Responses Are Phenotypically Exploitable. Neuron *108*, 1146–1162.e10. https://doi.org/10.1016/j.neuron.2020.09.021.

11. Nott, A., Holtman, I.R., Coufal, N.G., Schlachetzki, J.C.M., Yu, M., Hu, R., Han, C.Z., Pena, M., Xiao, J., Wu, Y., et al. (2019). Brain cell type-specific enhancer-promoter interactome maps and disease. Science *366*, 1134–1139. https://doi.org/10.1126/science.aay0793.

12. Mussa, Z., Tome-Garcia, J., Jiang, Y., Akbarian, S., and Tsankova, N.M. (2021). Isolation of Adult Human Astrocyte Populations from Fresh-frozen Cortex using Fluorescence-Activated Nuclei Sorting. J. Vis. Exp. https://doi.org/10.3791/62405.

13. Sun, W., Cornwell, A., Li, J., Peng, S., Osorio, M.J., Aalling, N., Wang, S., Benraiss, A., Lou, N., Goldman, S.A., and Nedergaard, M. (2017). SOX9 Is an Astrocyte-Specific Nuclear Marker in the Adult Brain Outside the Neurogenic Regions. J. Neurosci. *37*, 4493–4507. https://doi.org/10.1523/JNEUROSCI.3199-16.2017.

14. Channathodiyil, P., and Houseley, J. (2021). Glyoxal fixation facilitates transcriptome analysis after antigen staining and cell sorting by flow cytometry. PLoS One *16*, e0240769. https://doi.org/10.1371/journal.pone.0240769.

15. Andrews, S. (2010). FastQC: a quality control tool for high throughput sequence data. Available online: http://www.bioinformatics.babraham.ac.uk/projects/fastqc.

16. Dobin, A., Davis, C.A., Schlesinger, F., Drenkow, J., Zaleski, C., Jha, S., Batut, P., Chaisson, M., and Gingeras, T.R. (2013). STAR: ultrafast universal RNA-seq aligner. Bioinformatics *29*, 15–21. https://doi.org/10.1093/bioinformatics/bts635.

17. Robinson, J.T., Thorvaldsdóttir, H., Winckler, W., Guttman, M., Lander, E.S., Getz, G., and Mesirov, J.P. (2011). Integrative genomics viewer. Nat. Biotechnol. *29*, 24–26. https://doi.org/10.1038/nbt.1754.

18. Heinz, S., Benner, C., Spann, N., Bertolino, E., Lin, Y.C., Laslo, P., Cheng, J.X., Murre, C., Singh, H., and Glass, C.K. (2010). Simple combinations of lineage-determining transcription factors prime cis-regulatory elements required for macrophage and B cell identities. Mol. Cell *38*, 576–589. https://doi.org/10.1016/j.molcel.2010.05.004.

19. Hanzelmann, S., Castelo, R., and Guinney, J. (2013). GSVA: gene set variation analysis for microarray and RNA-seq data. BMC Bioinformatics *14*, 7. https://doi.org/10.1186/1471-2105-14-7.

20. Farhy-Tselnicker, I., Boisvert, M.M., Liu, H., Dowling, C., Erikson, G.A., Blanco-Suarez, E., Farhy, C., Shokhirev, M.N., Ecker, J.R., and Allen, N.J. (2021). Activity-dependent modulation of synapse-regulating genes in astrocytes. Elife *10*, e70514. https://doi.org/10.7554/eLife.70514.